Binding pathway of Tamiflu to ~~the active site of the~~ avian H5N1 neuraminidase

Hung T. Nguyen[§] and Thanh N. Truong[§]*

§ Life Science Laboratory, Institute for Computational Science and Technology, HCM city, Vietnam

* Department of Chemistry, University of Utah, Salt Lake city, Utah

Tienhungf91@gmail.com, Thanh.Truong@utah.edu

RECEIVED DATE (to be automatically inserted after your manuscript is accepted if required according to the journal that you are submitting your paper to)

ABSTRACT. Avian influenza has been causing great concern in the scientific community due to its rapid spread out and quick mutation rate. In this report, conventional docking method is employed in a novel way to obtain the binding pathway of Tamiflu (oseltamivir) into the avian influenza H5N1 neuraminidase binding pocket. Two pathways, one major and one minor, are revealed during this so-called pathway docking procedure. The two flexible 150 and 430 loops of the avian neuraminidase (N1) are found important in the process of guiding oseltamivir to get into the active site thanks to charge-charge and hydrogen bonding interactions. Moreover, particular interest is the role of D151 as the center for upturned movements of oseltamivir once it reaches the cavity annulus.

TOC GRAPHIC.

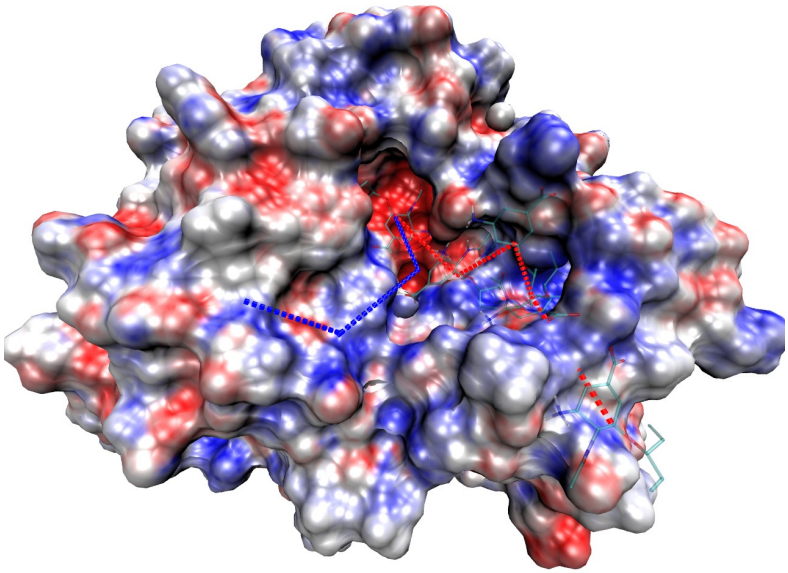

KEYWORDS. Pathway docking, Avian influenza, Tamiflu, Neuraminidase, H5N1.

INTRODUCTION

Avian influenza, especially subtype H5N1, with the ease of infection amongst birds and high rate of mutation remains the pandemic threat of the world.[1] (Add the impact of bird flu on the world economic as well).

The H5N1 Neuraminidase (N1), a glycoprotein supporting the release of new virions from infected cells to nearby healthy ones,[2] has a relatively well-conserved active site, thus has been theurapeutic target for antiviral structure-based drug design.[3,4] Tamiflu and Relenza are currently the first two FDA approved drugs widely used to treat the avian influenza.[2,5,6] Unfortunately, these types of~~such~~ virus ~~types~~ are known for their quick mutations and gene assortments which enable them to escape the host immune systems and cause drug resistance.[7,8] It has been still an unresolved debate of how known drug resistant mutations (H274Y, N294S) could affect the binding affinity of commercial drugs.[9-14] On the other hand, there have been several approaches proposing good candidates to be further optimized to become new drugs against N1.[15-21] Undoubtedly, understanding how the inhibitor advances and enters the active site, the so-called molecular recognition and docking processes, definitely assists this optimization procedure to achieve higher antiviral efficiency and avoid drug resistance.

Need to setup the problem a little better. Raise the issue why understanding the binding pathway such as the relative locations of the mutations from the active site, etc.

Let focus only on the host-guess binding pathway. Don't have to cover the reaction pathway, that will divert your discussion and focus. Reaction pathway has been widely used to study the mechanism of chemical reactions. This method provides a way to observe dynamically the system behavior from the reactants to the products. However, the conformational space that reaction pathway could sample is very limited since it needs to know exactly the conformations of the reactants and products, i.e. the two ends are fixed. In the case of complex biological systems, only one end, the crystallographic or docking structure of the complex, is known, therefore one has to search for a more powerful method.

Organize this discussion a little better: There are several approaches for determination of the binding pathway. These approaches are based on MD, MC, Brownian dynamics, ... Then provide description of each approach with its advantages and disadvantages as you did below. Simplify it a little bit.

Molecular dynamics (MD) contains time variable and thus can be used to study the way ligands get into or out of the binding pocket (reviewed in refs 22, 23). Unfortunately, the fact that ligands need to surpass so many high energy barriers along the pathway makes the current computational power is still far from one needed to get useful information. This could explain why until now, there have been very few efforts using conventional MD to study the binding pathway.[24-26] To speed up this process and reduce the computational cost, one approach is to introduce an external force to help the ligands go past these barriers more easily in Steered MD (SMD).[27,28] In this method, a force is applied onto a virtual atom connected to a real one, or in some cases to the center of mass of a molecular group, via a string. The ligand would consequently follow the virtual atom during the simulation and thus could far more easily get out of the binding pocket thanks to this external force. It is also used widely to study the extraction of lipids from membranes as well as the protein unfolding processes.[29-39] Yet, the problem one

has to face with when using this method to deal with binding pathway process is that the path obtained in this way is biased since one has to pick the direction and amplitude of the force which possibly causes artifact in data analysis.

To introduce a perturbation into the system, instead of an external force one could modify the force field itself. Targeted MD (TMD) proposed by Schlitter et al.[40-41] implements a time-dependent holonomic or harmonic constraint on the RMSD thus could drive a system to the target structure.[42-49] During the simulation, the system could implicitly "feel" and slowly evolve to the final state. A less prejudiced method is Biased MD (BMD)[50] in which the system would not feel any external perturbation if it moves towards the target, but the biasing potential would be turned on whenever it moves away from the target.[51,52] These two methods plus SMD are widely used to study transitional processes of biomolecules, sharing the common of introducing a perturbation to the system to drive it from a predefined to target state, but differing in how the perturbation is applied.[53] Still, locating the initial states to start with is remained one of the challenges when using these three methods. Also, the way people forces the system to behave as one wants makes them unrealistic and thus limits its accuracy.

Another recent approach is to combine directional guiding, Monte-Carlo search and minimization as proposed by Straber et al.[54] In this procedure, ligands are translated to the binding pocket on a virtual guiding line. At each steps, rotation over all defined rotatable bonds of the ligands and predetermined amino acids will be carried out and the structure of the whole complex will be consequently energy-minimized to obtain a new generation. With a similar direction, Ram et al. combine energy minimization and MD simulation to look for the binding pathway.[55] Ligands are moved incrementally from the pocket to the surface. At each of intermediate states, energy minimization and MD simulation are carried out. These two methods are quick ways to deal with the pathway problem, though they would be better used as refining rather than starting methods since one has to define an arbitrary "guiding line" from outside to the pocket.

Brownian dynamics has been also one tool studying the diffusion and transport phenomena, as well as the molecular recognition and binding processes.[56-58] These would need supporting evidences from experiments to stand firmly for their predictions.

Describe the idea in one short paragraph with the motivation and reasoning.

In this letter, we implement the docking method in a novel way in order to obtain the drug pathway. Docking has been conventionally used to find the optimal position of ligands inside the active site or recreate the experimental structure of the complex.[59-64] The idea is if we could find best places to put the ligand in each locally regional space then we hope to construct the path from such discrete poses. Certainly, one should treat the pathway problem using the kinetics viewpoint in stead of thermodynamics like this. However, due to the computational unfeasibility of such approaches we have to assume that these minima contribute most of the minima in the potential energy surface. All the rest of the path (the "reaction coordinate", the "transition states") could be afterwards built up using structures from these minima using the other advanced techniques. This approach avoids initial biases of locating the starting point and choosing the direction which the ligand follows. Essentially, we used AutoDock 4.2.1[65] to sample each regional space, one by one gets closer to the binding pocket. The coordinates of the clusters were analyzed to find out all possible pathways. The major path would be consequently refined further using the same technique, but in smaller boxes along the path to obtain a smoother one. Move some of the computational details here to the section below.

COMPUTATIONAL DETAILS

To include the protein flexibility in this pathway docking procedure, we did clustering analysis as in Daura et al.[66] to extract the most representative ensembles from a 40 ns molecular dynamics trajectory. The two top ensembles which represented nearly half of the whole trajectory (45%) were used as receptors in the pathway docking process to guarantee most of the conformational space is incorporated.

The best clusters in each box are likely to form a path from outside to the binding pocket. In addition, there is also another minor one formed by smaller clusters, yet predominated by the major path. To get a

smoother one, we defined several small (but enough for Tamiflu to fully extend) boxes along the major path and did docking again with the same parameters except the number of dockings of 100 due to the reduction in space sampling.

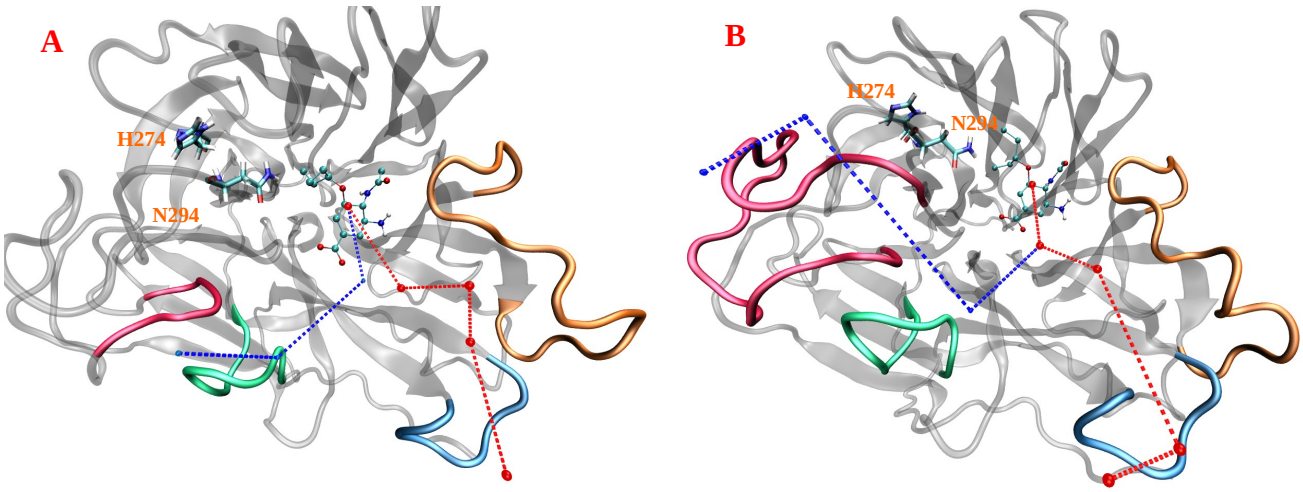

Figure 1. Binding pathway of Tamiflu obtained for the two most representative receptors, first (A) and second (B). The major path is encoded in red dashed line whereas the blue represents the minor one. Some loops predicted to be important in the binding process are also shown: 150-orange, 430-cyan, 370-green, 340-pink. Two likely mutated residues (H274 and N294) are depicted in bonds for reference.

RESULTS

As clearly seen in Fig. 1A made with VMD[67], the major path is very close to the 430 and 150-loop. Since these two loops were observed flexible during the MD simulation,[68] the path obtained could vary significantly. To check this hypothesis, we also performed the same pathway docking protocol using the second most representative ensemble receptor. Of note, the differences between two major paths are negligible though the conformations of two 150 and 430 loops are quite different from the former when one moves to the second. This confirms strongly that oseltamivir gets into the active site thanks much to the contacts it makes with 150 and 430 loops.

Table 1. Binding free energy along the pathway calculated using the docking program Autodock when oseltamivir advances the pocket of the two most representative clusters of N1.

Step	E_{bind} (kcal/mol)	
	Receptor_1	Receptor_2

	Major path	Minor path	Major path	Minor path
1	- 3.43	- 4.61	- 2.75	- 4.04
2	- 3.70	- 4.70	- 4.22	- 4.53
3	- 5.07	- 5.79	- 5.07	- 4.98
4	- 6.00		- 6.41	- 6.41
Binding pose	- 8.46		- 8.27	

The binding free energy along the pathway was stably decreased step by step as oseltamivir penetrated the active site. Certainly, these free binding energies were not quite accurate since the scoring function of Autodock was built by fitting the parameters to reproduce the energy of ligands inside the pocket. Therefore, to obtain more precise energies one should use force-field based scoring function instead or even more robust methods such as MM/PBSA, TI or FEP.

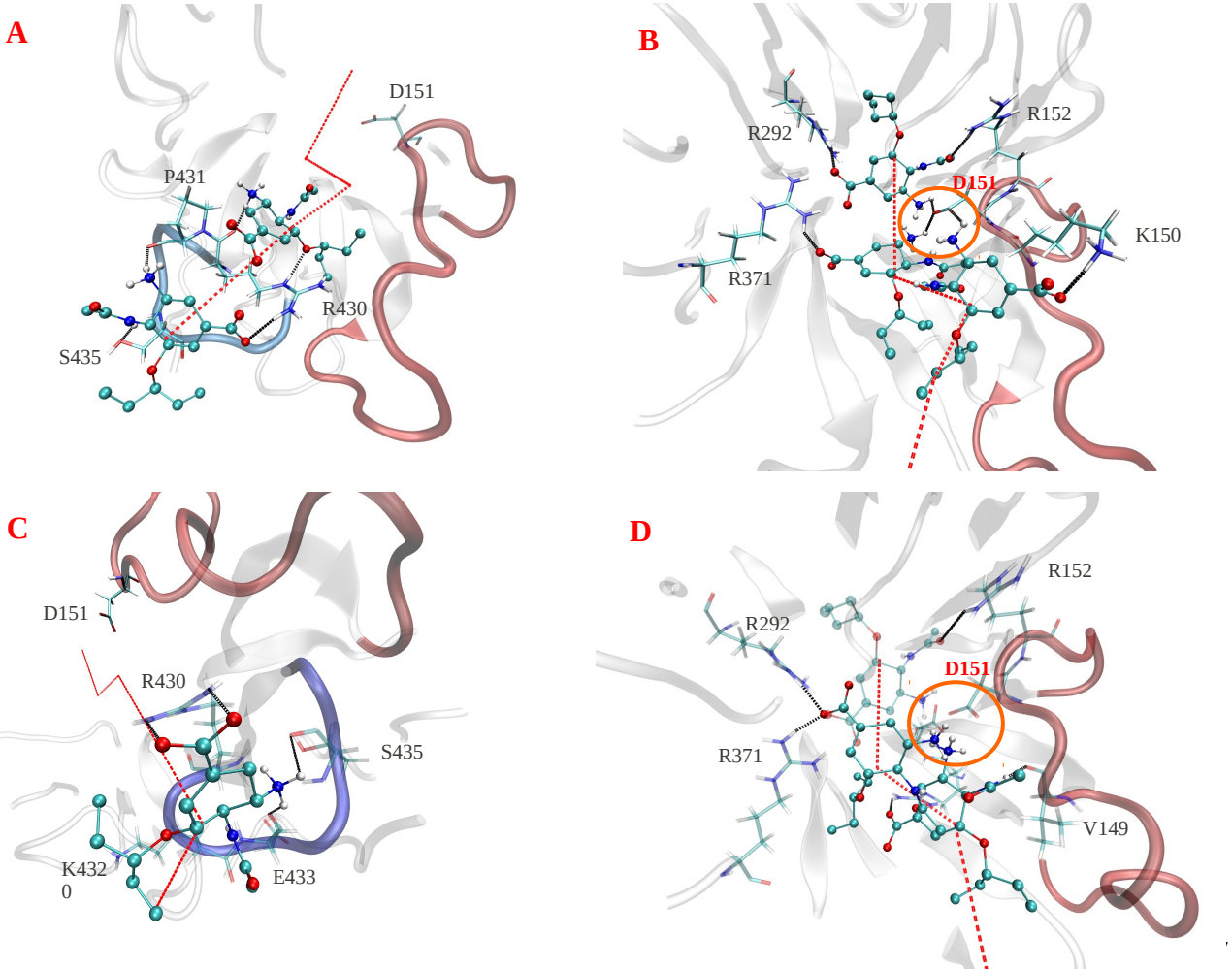

Figure 2. Hydrogen bond network between oseltamivir (shown in CPK) and key residues (shown in bonds) in the major path. (A), (B): from outside to inside, respectively, of the top ensemble receptor while (C), (D) are counterparts for the second receptor. 150-loop is depicted in pink, while 430-loop is represented in blue.

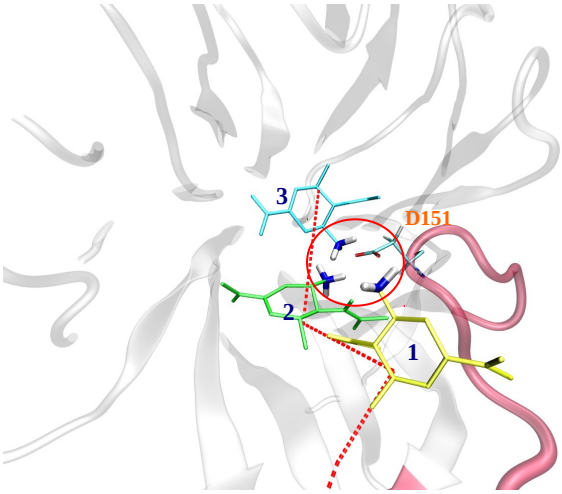

Figure 3. The role of carboxylate group of D151 (shown in bonds) in the binding process of oseltamivir to the avian neuraminidase. The cores of oseltamivir (without pentyl moiety) are depicted in different colors corresponding to the final steps in the docking process to the active site.

Detailed analysis of intermolecular hydrogen bonds between oseltamivir and NA reveals an unexpected role of D151. This residue guards the entrance of the binding pocket and thus oseltamivir very soon makes contact with it while reaching the active site. As shown in Fig. 2B, 2D and 3, the amino group (NH_3^+) of oseltamivir interacts strongly with the carboxylate group (COO^-) of D151. It is unclear that whether the oseltamivir's amino group remains at the same position making contact with D151 once it reaches the active site since in both cases it is likely to rotate about this positively charged group to approach the binding pose. Further investigations would be required to obtain a more detailed answer of oseltamivir's behavior once it reached the cavity annulus.

Of note, the binding path has no contact with the two known likely mutated residues N294 and H274 that lie on the opposite side of where the 150 and 430 loops locate. Several studies have proposed

mechanisms of drug resistance relating to these two residues. H274Y was suspected to disrupt the interactions between oseltamivir with R152 and to reduce the size of the hydrophobic pocket near the oseltamivir's pentyl moiety.[11,13,14] However, there has been much debate on the N294S resistant mechanism. An interesting approach by Le et al. suggested that N294 conspicuously lied on the "negatively charged pathway" which guided directly to binding pocket.[13] To clarify whether our paths are consistent with this suggestion, electrostatic potentials are calculated using APBS 1.2[69] and mapped onto the surface of N1 as illustrated in Fig. 4.

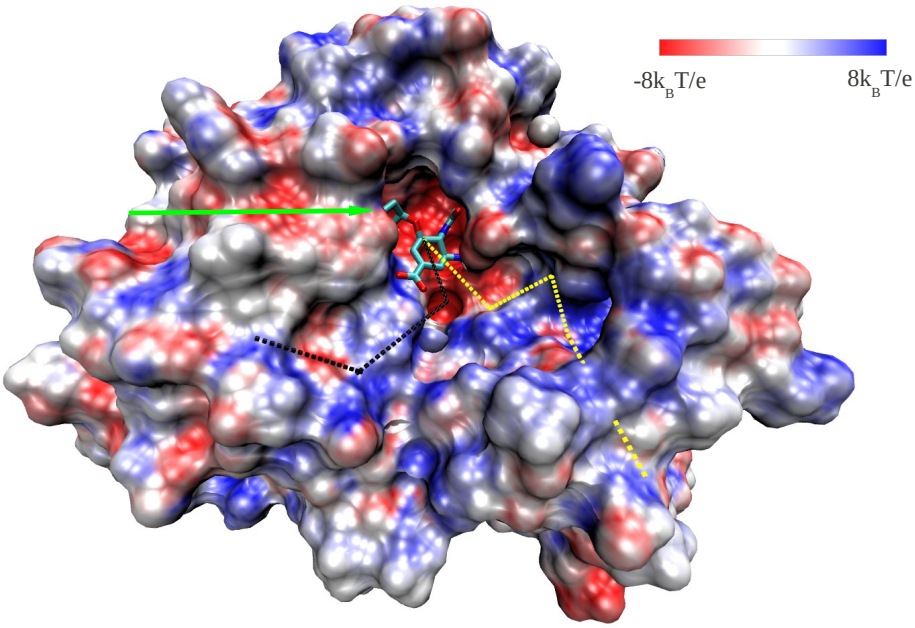

Figure 4. Electrostatic surface potentials of avian influenza H5N1 Neuraminidase with oseltamivir bound inside the cavity. Also shown are two binding pathways found in this letter, major (yellow) and

minor one (black). The “negatively charged pathway” as suggested in Le et al. is depicted by a green arrow.

The binding pocket is highly negatively charged thus it is at first reasonable to speculate oseltamivir would be guided to the active site by such a negative pathway. However, more careful thoughts have shown that besides positive group (NH_3^+), oseltamivir also has negatively charged moieties (COO^- and CO) and they do make contacts with positive guanidinium groups of R152, R292 and R371 in the pocket. This fact arouses the possibility that it is not necessary for oseltamivir to follow the “negatively charged pathway” since it could utilize these negative moieties instead of the positive NH_3^+ when approaching the binding cavity. This hypothesis is strongly supported by the hydrogen bond analysis above since important interactions are mostly established from the COO^- group of oseltamivir.

Clearly, using docking method to study conformational changes would have many inevitable drawbacks. The water molecules were treated implicitly and thus contacts between drugs and solvents as well as the exfiltration of water molecules whenever there was a drug penetrating into the active site were unavoidably excluded. The protein flexibility that was important during the binding process was also omitted and thus to incorporate water movement and protein flexibility explicitly one should employ perturbation MD methods such as SMD, TMD or BMD or other hybrid methods. Furthermore, the scoring function of Autodock was empirical and fitted to reproduce the binding free energy inside the pocket and therefore was not suitable for describing the system when the ligand was relatively far from the binding poses. In this case, such scoring functions like force-field based ones were believed to treat the complexes better and give the free energy more precisely.

Utilizing the conventional docking method, we have found that there were two ways for oseltamivir to advance to the binding pocket of avian influenza H5N1 neuraminidase. The two well-known 150 and 430 loops have been found to play important roles in guidance the drug to the binding pose despite their considerable flexibility. D151’s role of the center for upturned movement of oseltamivir has been unexpectedly revealed during this pathway docking procedure. Our two pathways are also not identical

with the so-called “negatively charged pathway” recently suggested by Le et al. and thus further both experimental and theoretical studies to provide more supporting evidences would be more than helpful.

ACKNOWLEDGMENT. We thank the Ho Chi Minh City government for their support of the Institute for Computational Science and Technology (ICST) and the ICST staffs for their technical help.

Supporting Information Available. Materials and methods including clustering analysis, docking parameters, ranking the clusters; a figure of boxes used in docking process; a table ranking clusters obtained in the docking process; a figure of hydrogen bonds in the minor pathway. This material is available free of charge via the Internet at http://pubs.acs.org.

References

1. Abdel-Ghafar, A. N.; Chotpitayasunondh, T.; Gao, Z.; Hayden, F. G.; Nguyen, D. H.; de Jong, M. D.; Naghdaliyev, A.; Peiris, J. S.; Shindo, N.; Soeroso, S.; Uyeki, T. M. Update on avian influenza A (H5N1) virus infection in humans. *N. Engl. J. Med*. **2008**, *358* (3), 261-273.

2. Colman, P. Anti-influenza drugs from neuraminidase inhibitors. In *Structure-based drug discovery: An overview*; Hubbard, R. E., Ed.; Royal Society of Chemistry; Cambridge, 2006.

3. De Clercq, E. Antiviral agents active against influenza A viruses. *Nat. Rev. Drug Discov.* **2006**, *5*, 1015-1025.

4. De Clercq, E.; Neyts, J. Avian influenza (H5N1) infection: targets and strategies for chemotherapeutic intervention. *Trends Pharmacol. Sci.* **2007**, *28* (6), 280-285.

5. Lew, W.; Chen, X.; Kim, C. U. Discovery and development of GS 4104 (oseltamivir): an orally active influenza neuraminidase inhibitor. *Curr. Med. Chem.* **2000**, *7* (6), 663-672.

6. von Itzstein, M.; Wu, W. Y.; Kok, G. B.; Pegg, M. S.; Dyason, J. C.; Jin, B.; Phan, T. V.; Smythe, M. L.; White, H. F.; Oliver, S. W.; Colman, P. M.; Varghese, J. N.; Ryan, D. M.; Woods, J. M.; Bethell, R. C.; Hotham, V. J.; Cameron, J. M.; Penn, C. R. Rational design of potent sialidase-based inhibitors of influenza virus replication. *Nature* **1993**, *363*, 418-423.

7. Beigel, J. H.; Farrar, J.; Han, A. M.; Hayden, F. G.; Hyer, R.; de Jong, M. D.; Lochindarat, S.; Nguyen, T. K.; Nguyen, T. H.; Tran, T. H.; Nicoll, A.; Touch, S.; Yuen, K. Y. Avian influenza (H5N1) infection in humans. *N. Engl. J. Med.* **2005**, *353* (13), 1374-1385.

8. de Jong, M. D.; Tran, T. T.; Truong, H. K.; Vo, M. H.; Smith, G. J.; Nguyen, V. C.; Bach, V. C.; Phan, T. Q.; Do, Q. H.; Guan, Y.; Peiris, J. S.; Tran, T. H.; Farrar, J. Oseltamivir resistance during treatment of influenza A (H5N1) infection. *N. Engl. J. Med*. **2005**, *353* (25), 2667-2672.

9. Collins, P. J.; Haire, L. F.; Lin, Y. P.; Liu, J.; Russell, R. J.; Walker, P. A.; Skehel, J. J.; Martins, S. R.; Hay, A. J.; Gamblin, S. J. Crystal structures of oseltamivir-resistant influenza virus neuraminidase mutants. *Nature* **2008**, *453* (7199), 1258-1261.

10. Wang, N. X.; Zheng, J. J. Computational studies of H5N1 influenza virus resistance to oseltamivir. *Protein Sci.* **2009**, *18* (4), 707-715.

11. Malaisree, M.; Rungrotmongkol, T.; Nunthaboot, N.; Aruksakunwong, O.; Intharathep, P.; Decha, P.; Sompornpisut, P.; Hannongbua, S. Source of oseltamivir resistance in avian influenza H5N1 virus with the H274Y mutation. *Amino Acids* **2009**, *37* (4), 725-732.

12. Rungrotmongkol, T.; Udommaneethanakit, T.; Malaisree, M.; Nunthaboot, N.; Intharathep, P.; Sompornpisut P.; Hannongbua, S. How does each substituent functional group of

oseltamivir lose its activity against virulent H5N1 influenza mutants? *Biophys. Chem.* **2009**, *145*, 29-36.

13. Le, L.; Lee, E. H.; Hardy, D. J.; Truong, T. N.; Schulten, K. Electrostatic funnel directs binding of Tamiflu to H5N1/H1N1pdm neuraminidase. *PLoS Comput. Biol.* **2010**, submitted.

14. Park, J. W.; Jo, W. H. Infiltration of water molecules into the oseltamivir-binding site of H274Y neuraminidase mutant causes resistance to oseltamivir. *J. Chem. Inf. Model.* **2009**, *49* (12), 2735-2741.

15. Cheng, L. S.; Amaro, R. E.; Xu, D.; Li, W. W.; Arzberger, P. W.; McCammon, J. A. Ensemble-based virtual screening reveals potential novel antiviral compounds for avian influenza neuraminidase. *J. Med. Chem.* **2008**, *51*, 3878-3894.

16. An, J.; Lee, D. C. W.; Law, A. H. Y.; Yang, C. L. H.; Poon, L. L. M.; Lau, A. S. Y.; Jones, S. J. M. A novel small-molecule inhibitors of the avian influenza H5N1 virus determined through computational screening against the neuraminidase. *J. Med. Chem.* **2009**, *52* (9), 2667-2672.

17. Garcia-Sosa, A. T.; Sild, S.; Maran, U. Design of multi-binding-site inhibitors, ligand efficiency, and consensus screening of avian influenza H5N1 wild-type neuraminidase and of the oseltamivir-resistant H274Y variant. *J. Chem. Inf. Model.* **2008**, *48* (10), 2074-2080.

18. Macdonald, S. J. F.; Cameron, R.; Demaine, D. A.; Fenton, R. J.; Foster, G.; Gower, D.; Hamblin, J. N.; Hamilton, S.; Hart, G. J.; Hill, A. P.; Inglis, G. G. A.; Jin, B.; Jones, H. T.; McConnell, D. B.; McKimm-Breschkin, J.; Mills, G.; Nguyen, V.; Owens, I. J.; Parry, N.; Shanahan, S. E.; Smith, D.; Watson, K. G.; Wu, W.;Tucker, S. P. Dimeric zanamivir

conjugates with various linking groups are potent, long-lasting inhibitors of influenza neuraminidase including H5N1 avian influenza. *J. Med. Chem.* **2005**, *48* (8), 2964-2971.

19. Grienke, U.; Schmidtke, M.; Kirchmair, J.; Pfarr, K.; Wutzler, P.; Durrwald, R.; Wolber, G.; Liedl, K. R.; Stuppner, H.; Rollinger, J. M. Antiviral potential and molecular insight into neuraminidase inhibiting diarylheptanoids from Alpinia katsumadai. *J. Med. Chem.* **2010**, *53* (2), 778-786.

20. Abu, A. M.; Taha, M. O. Pharmocophore modeling, quantitative structure-activity relationship analysis, and shape-complemented in silico screening allow access to novel influenza neuraminidase inhibitors. *J. Chem. Inf. Model.* **2009**, *49* (4), 978-996.

21. Park, J. W.; Jo, W. H. Computational design of novel, high-affinity neuraminidase inhibitors for H5N1 avian influenza virus. *Eur. J. Med. Chem.* **2010**, *45* (2), 536-541.

22. van Gunsteren, W. F.; Berendsen, H. J. C. Computer simulation of molecular dynamics: Methodology, applications, and perspectives in chemistry. *Angew. Chem. Int. Ed. Engl.* **1990**, *29*, 992-1023.

23. Karplus, M.; Petsko, G. A. Molecular dynamics simulations in biology. *Nature* **1990**, *347*, 631-639.

24. Hofacker, I.; Schulten, K. Oxygen and proton pathways in cytochrome c oxidase. *Proteins: Str. Funct. Genet.* **1998**, *30*, 100-107.

25. Ruscio, J. Z.; Kumar, D.; Shukla, M.; Prisant, M. G.; Murali, T. M.; Onufriev, A. V. Atomic level computational identification of ligand migration pathways between solvent and binding site in myoglobin. *Proc. Natl. Acad. Sci.* **2008**, *105* (27), 9204-9209.

26. Baron, R.; Riley, C.; Chenprakhon, P.; Thotsaporn, K.; Winter, R. T.; Alfieri, A.; Forneris, F.; van Berkel, W. J. H.; Chaiyen, P.; Fraaije, M. W.; Mattevi, A.; McCammon, J. A. Multiple pathways guide oxygen diffusion into flavoenzyme active sites. *Proc. Natl. Acad. Sci.* **2009**, *106* (26), 10603-10608.

27. Grubmuller, H.; Heymann, B.; Tavan, P. Ligand binding: molecular mechanics calculation of the streptavidin-biotin rupture force. *Science* **1996**, *271*, 997-999.

28. Sotomayor, M.; Schulten, K. Single-molecule experiments in vitro and in silico. *Science* **2007**, *316*, 1144-1148.

29. Izrailev, S.; Stepaniants, S; Balsera, M.; Oono, Y.; Schulten, K. Molecular dynamics study of unbinding of the avitin-biotin complex. *Biophys. J.* **1997**, *72*, 1568-1581.

30. Isralewitz, B.; Izrailev, S.; Schulten, K. Binding pathway of retinal to bacterio-opsin: a prediction by molecular dynamics simulations. *Biophys. J.* **1997**, *73* (3), 2972-2979.

31. Kosztin, D.; Izrailev, S.; Schulten, K. Unbinding of retinoic acid from its receptor studied by steered molecular dynamics. *Biophys. J.* **1999**, *76* (1), 188-197.

32. Ludermann, S. K.; Lounnas, V.; Wade, R. C. How do substrates enter and products exit the buried active site of cytochrome P450cam? 2. Steered molecular dynamics and adiabatic mapping of substrate pathways. *J. Mol. Biol.* **2000**, *303* (5), 813-830.

33. Xu, Y.; Shen, J.; Luo, X.; Silman, I.; Sussman, J. L.; Chen, K.; Jiang, H. How does Huperzine A enter and leave the binding gorge of Acetylcholinesterase? Steered molecular dynamics simulations. *J. Am. Chem. Soc.* **2003**, *125* (37), 11340-11349.

34. Yang, L. J.; Zou, J.; Xie, H. Z.; Li, L. L.; Wei, Y. Q.; Yang, S. Y. Steered molecular dynamics simulations reveal the likelier dissociation pathway of Imatinib from its targeting kinases c-Kit and Abl. *PLoS One* **2009**, *4* (12): e8470. doi:10.1371/journal.pone.0008470.

35. Stepaniants, S.; Izrailev, S.; Schulten, K. Extraction of lipids from phospholipid membranes by steered molecular dynamics. *J. Mol. Model.* **1997**, *3*, 473-475.

36. Jensen, M. O.; Yin, Y.; Tajkhorshid, E.; Schulten, K. Sugar transport across lactose permease probed by steered molecular dynamics. *Biophys. J.* **2007**, *93* (1), 92-102.

37. Lu, H.; Isralewitz, B.; Krammer, A.; Vogel, V.; Schulten, K. Unfolding of titin immunoglobulin domains by steered molecular dynamics simulation. *Biophys. J.* **1998**, *75*, 662-671.

38. Grater, F.; Shen, J.; Jiang, H.; Gautel, M.; Grubmuller, H. Mechanically induced titin kinase activation studied by force-probe molecular dynamics simulations. *Biophys. J.* **2005**, *88*, 790-804.

39. Isralewitz, B.; Gao, M.; Schulten, K. Steered molecular dynamics and mechanical functions of proteins. *Curr. Opin. Struct. Biol.* **2001**, *11* (2), 224-230.

40. Schlitter, J.; Engels, M.; Kruger, P.; Jacoby, E. U.; Wollmer, A. Targeted molecular dynamics simulation of conformational change: application to the T-R transition in insulin. *Mol. Sim.* **1993**, *10*, 291-308.

41. Schlitter, J.; Engels, M.; Kruger, P. Targeted molecular dynamics: a new approach for searching pathways of conformational transitions. *J. Mol. Graph.* **1994**, *12*, 84-89.

42. Ma, J.; Karplus, M. Molecular switch in signal transduction: Reaction paths of the conformational changes in ras p21. *Proc. Natl. Acad. Sci.* **1997**, *94*, 11905-11910.

43. Ma, J.; Sigler, P. B.; Xu, Z.; Karplus, M. A dynamic model for the allosteric mechanism of GroEL. *J. Mol. Biol.* **2000**, *302*, 303-313.

44. Barrios, F. R.; Balzarini, J.; Gago, F. The molecular basis of resilience to the effect of the Lys103Asn mutation in non-nucleoside HIV-1 Reverse Transcriptase inhibitors studied by targeted molecular dynamics simulations. *J. Am. Chem. Soc.* **2005**, *127*, 7570-7578.

45. Mashl, R. J.; Jakobsson, E. End-point targeted molecular dynamics: Large-scale conformational changes in potassium channels. *Biophys. J.* **2008**, *94*, 4307-4319.

46. Ferrara, P.; Apostolakis, J.; Caflisch, A. Targeted molecular dynamics simulations of protein unfolding. *J. Phys. Chem. B* **2000**, *104* (18), 4511-4518.

47. Mendieta, J.; Gago, F.; Ramirez, G. Binding of 5'-GMP to the GluR2 AMPA receptor: Insight from targeted molecular dynamics simulations. *Biochemistry* **2005**, *44* (44), 14470-14476.

48. Perdih, A.; Kotnik, M.; Hodoscek, M.; Solmajer, T. Targeted molecular dynamics simulation studies of binding and conformational changes in E.coli MurD. *Proteins: Str. Funct. Genet.* **2007**, *68* (1), 243-254.

49. Cheng, X.; Wang, H.; Grant, B.; Sine, S. M.; McCammon, J. A. Targeted molecular dynamics study of C-loop closure and channel gating in nicotinic receptors. *PLoS Comput. Biol.* **2006**, *2* (9): e134. doi:10.1371/journal.pcbi.0020134.

50. Marchi, M.; Ballone, P. Adiabatic bias molecular dynamics: A method to navigate the conformational space of complex molecular systems. *J. Chem. Phys.* **1999**, *110* (8), 3697.

51. Paci, E.; Caflisch, A.; Pluckthun, A.; Karplus, M. Forces and energetics of hapten-antibody dissociation: a biased molecular dynamics simulation study. *J. Mol. Biol.* **2001**, *314* (3), 589-605.

52. Morra, G.; Hodoscek, M.; Knapp, E. W. Unfolding of the cold shock protein studied with biased molecular dynamics. *Proteins: Str. Funct. Genet.* **2003**, *53* (3), 597-606.

53. Huang, H.; Ozkirimli, E.; Post, C. B. Comparison of three perturbation molecular dynamics methods for modeling conformational transitions. *J. Chem. Theory Comput.* **2009**, *5* (5), 1304-1314.

54. Straber, A.; Wittmann, H. LigPath: a module for predictive calculation of a ligand's pathway into a receptor-application to the gpH1 – receptor. *J. Mol. Model.* **2007**, *13*, 209-218.

55. Sai Ram, K. V. V. M.; Rambabu, G.; Sarma, J. A. R. P.; Desiraju, G. R. Ligand coordinate analysis of SC-558 from the active site to the surface of COX-2: a molecular dynamics study. *J. Chem. Inf. Model.* **2006**, *46* (4), 1784-1794.

56. Allison, S. A.; McCammon, J. A. Transport properties of rigid and flexible macromolecules by Brownian dynamics simulation. *Biopolymers* **1984**, *23*, 167-187.

57. Northrup, S. H.; Allison, S. A.; McCammon, J. A. Brownian dynamics of diffusion-influenced bimolecular reactions. *J. Chem. Phys.* **1984**, *80*, 1517-1524.

58. Allison, S. A.; McCammon, J. A. Dynamics of substrate binding to copper zinc superoxide dismutase. *J. Phys. Chem.* **1985**, *89*, 1072-1074.

59. Kitchen, D. B.; Decornez, H.; Furr, J. R.; Bajorath, J. Docking and scoring in virtual screening for drug discovery: methods and applications. *Nat. Rev. Drug Discov.* **2004**, *3*, 935-949.

60. Walters, W. P.; Stahl, M. L.; Murcko, M. A. Virtual screening – an overview. *Drug Discov. Today* **1998**, *3*, 160-178.

61. Gohlke, H.; Klebe, G. Appoaches to the description and prediction of the binding affinity of small-molecule ligands to macromolecule receptors. *Angew. Chem. Int. Ed.* **2002**, *41*, 2644-2676.

62. Brooijmans, N.; Kuntz, I. D. Molecular recognition and docking algorithms. *Annu. Rev. Biophys. Biolmol. Struct.* **2003**, *32*, 335-373.

63. Halperin, I.; Ma, B.; Wolfson, H.; Nussinov, R. Principles of docking: an overview of search algorithms and a guide to scoring functions. *Proteins: Str. Funct. Genet.* **2002**, *47*, 409-443.

64. Taylor, R. D.; Jewsbury, P. J.; Essex, J. W. A review of protein-small molecule docking methods. *J. Comput. Aided Mol. Des.* **2002**, *16* (3), 151-166.

65. Morris, G. M.; Goodsell, D. S.; Halliday, R. S.; Huey, R.; Hart, W. E.; Belew, R. K.; Olson, A. J. Automated docking using a Lamarckian genetic algorithm and an empirical binding free energy function. *J. Comp. Chem.* **1998**, *19* (14), 1639-1662.

66. Daura, X.; Gademann, K.; Jaun, B.; Seebach, D.; van Gunsteren, W. F.; Mark, A. E. Peptide folding: When simulation meets experiment. *Angew. Chem. Int. Ed.* **1999**, *38* (1-2), 236-240.

67. Humphrey, W.; Dalke, A.; Schulten, K. VMD – Visual Molecular Dynamics. *J. Mol. Graph.* **1996**, *14* (1), 33-38.

68. Amaro, R. E.; Minh, D. D.; Cheng, L. S.; Lindstrom, W. M., Jr.; Olson, A. J.; Lin, J. H.; Li, W. W.; McCammon, J. A. Remarkable loop flexibility in avian influenza N1 and its implications for antiviral drug design. *J. Am. Chem. Soc.* **2007**, *129* (25), 7764-7765.

69. Baker, N. A.; Sept, D.; Joseph, S.; Holst, M. J.; McCammon, J. A. Electrostatics of nanosystems: application to mictotubules and the ribosome. *Proc. Natl. Acad. Sci.* **2001**, *98*, 10037-10041.

How Tamiflu enters the active site of the avian H5N1 neuraminidase?

Hung T. Nguyen[§] and Thanh N. Truong[§]*

§ Life Science Laboratory, Institute for Computational Science and Technology, HCM city, Vietnam

* Department of Chemistry, University of Utah, Salt Lake city, Utah

Supporting information

Materials and Methods

Details of the MD simulation were given in our previous report.[1] Clustering analysis was done using the g_cluster tool in Gromacs package[2] on a subset of residues that lie in or near the binding pocket,[3] namely 117-119, 133-138, 146-152, 156, 179, 180, 196-200, 223-228, 243-247, 277, 278, 293, 295, 344-347, 368, 401, 402, and 426-441 with a cutoff of 1.4 Å. The top two centroids which represent nearly a half (44.8%) of the whole 40 ns trajectory were used as receptors in the pathway docking.

AutoDockTools 1.5.2[4] was used to add polar hydrogens, assign Gasteiger charges[5] and create grid binding boxes. To allow sufficient sampling and avoid loss of important minima due to artificial boundary condition, each box was constructed to overlap with the neighborings three fourth its depth. In addition, each box covered large space of 48 x 48 x 10.5 Å to guarantee that all possibility of entering the pocket was incorporated and full extension of Tamiflu was permitted. AutoGrid version 4.2.1 was used to calculate the binding affinities using the following atom types as in Tamiflu: C, NA (hydrogen bond accepting N), OA (hydrogen bond accepting O), HD (polar hydrogen), and two additional ones e (electrostatics) and d (desolvation map).

Lamarckian genetic algorithm was used to do the docking experiments using AutoDock 4.2.1.[6] Docking parameters were as follows: trials of 200 dockings, population size of 200, random starting position and conformation, translation step range of 2.0 Å, rotation step range of 50 degrees, maximum number of generations of 27000, elitism of 1, mutation rate of 2%, crossover rate of 80%, local search rate of 6%, 10 million energy evaluations, unbound model was “same as bound”, and docked conformations were clustered with the tolerance of 2.0 Å RMSD.

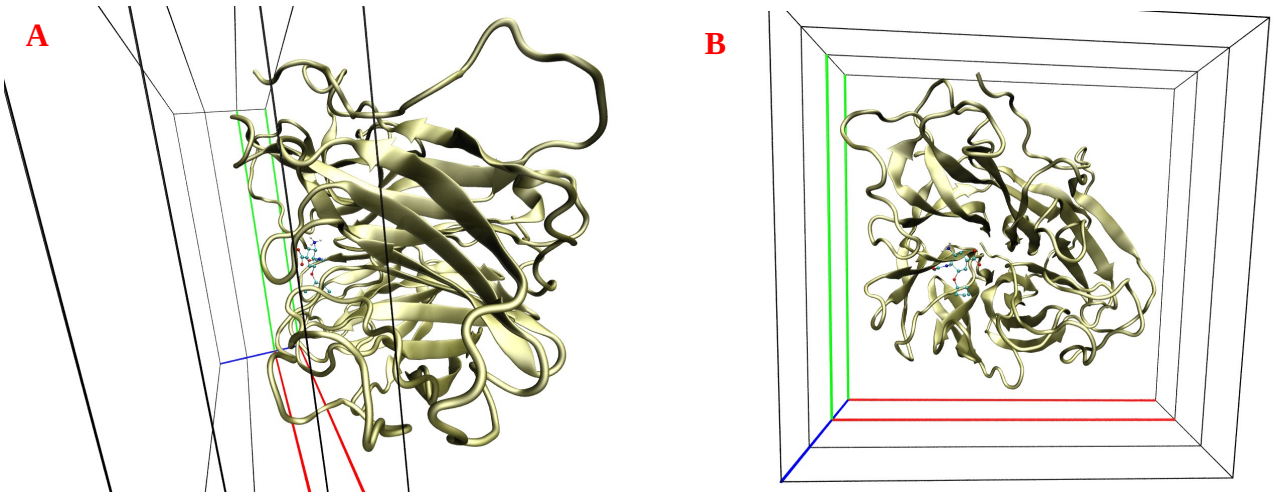

Figure S1. Boxes used in the pathway docking protocol. These boxes covered a large area and thus guaranteed full extension of Tamiflu and any possible direction towards the binding pocket.

To rank the clusters, we calculated the probability of cluster appearance in each box

$$N_i^j = \frac{n_i^j e^{-\frac{E_i^j}{RT}}}{\sum_i n_i^j e^{-\frac{E_i^j}{RT}}}$$

where n_i^j , E_i^j , N_i^j are the population, the lowest binding energy and the probability of finding cluster i in box j, respectively

R is the ideal gas constant and T is the temperature (298.15K).

Table S1. The most probable clusters in each box from the initial docking results against the most representative ensemble receptor, sorted with the appearance probability. Red numbers are corresponding to major path whereas blue ones are the minor.

Box	Ranking	$E_{binding}$ (kcal/mol)	Population	Probability (%)
1	1	-3.43	36	62.26
	2	-2.67	26	12.47
2	1	-3.70	32	41.32
	2	-3.59	9	9.65
	3	-3.20	17	9.44
3	1	-4.61	59	63.03
	2	-4.20	21	11.23
4	1	-5.04	104	75.80
	2	-4.70	25	10.26
5	1	-6.00	70	52.70
	2	-5.79	63	33.28
6	1	-8.44	65	89.72
	2	-6.71	117	8.71
7	1	-8.46	196	100.00

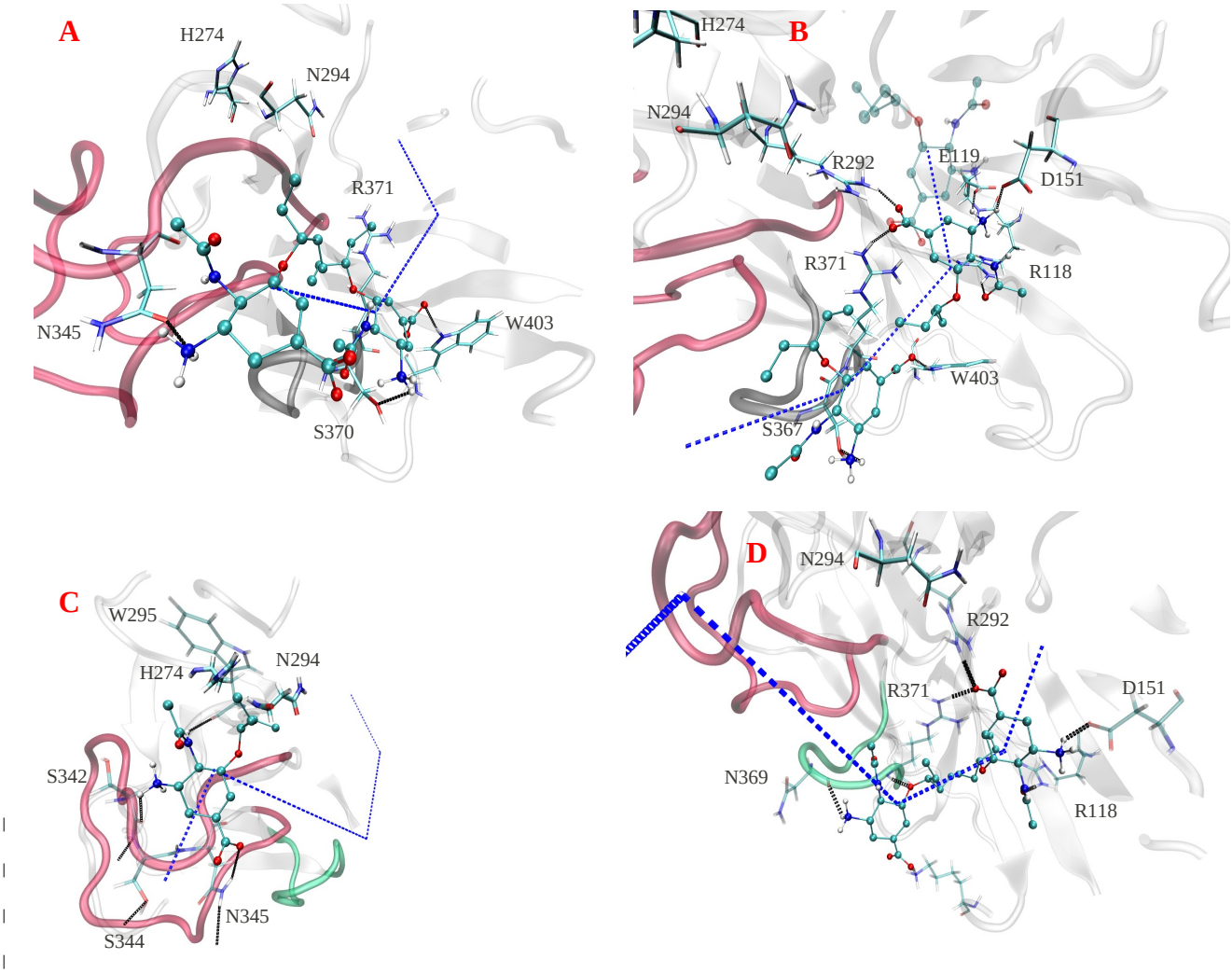

Figure S2. Hydrogen bond network between Tamiflu (shown in CPK) and key residues (shown in bonds) in the minor path (the dashed blue line). (A), (B): from outside to inside, respectively, of the top ensemble receptor while (C), (D) are counterparts for the second receptor. 340-loop is depicted in pink, while 370-loop is represented in green or grey.

References

1. Le, L.; Lee, E.; Hardy, D.; Schulten, K.; Truong, T. N. Molecular modeling of mutation-induced Tamiflu drug resistance for swine influenza H1N1pdm and avian H5N1 influenza N1 neuraminidase. *J. Mol. Med.* **2009**, submitted.

2. Hess, B.; Kutzner, C.; van der Spoel, D.; Lindahl, R. GROMACS 4: Algorithms for highly efficient, load-balanced, and scalable molecular simulation. *J. Chem. Theory Comput.* **2008**, *4* (3), 435-447.

3. Cheng, L. S.; Amaro, R. E.; Xu, D.; Li, W. W.; Arzberger, P. W.; McCammon, J. A. Ensemble-based virtual screening reveals potential novel antiviral compounds for avian influenza neuraminidase. *J. Med. Chem.* **2008**, *51*, 3878-3894.

4. Sanner, M. F. A component-based software environment for visualizing large macromolecular assemblies. *Structure* **2005**, *13* (3), 447-462.

5. Gasteiger, J.; Marsili, M. Iterative partial equalization of orbital electronegativity: a rapid access to atomic charges. *Tetrahedron* **1980**, *36* (22), 3219-3228.

6. Morris, G. M.; Goodsell, D. S.; Halliday, R. S.; Huey, R.; Hart, W. E.; Belew, R. K.; Olson, A. J. Automated docking using a Lamarckian genetic algorithm and an empirical binding free energy function. *J. Comp. Chem.* **1998**, *19* (14), 1639-1662.